Chemical Au-Au bonding induced by UV irradiation of dinuclear Gold(I) complexes. A computational study with experimental evidence.

Journal:	*Physical Chemistry Chemical Physics*
Manuscript ID:	CP-ART-09-2014-003990.R1
Article Type:	Paper
Date Submitted by the Author:	03-Oct-2014
Complete List of Authors:	Latouche, Camille; Université de Rennes 1, Sciences Chimiques de Rennes UMR 6226 CNRS Lin, Yan-Ru; National Dong Hwa Uiversity, chemistry Tobon, Yeny; Universite de Lille 1, LASIR Furet, Eric; UMR 6226, Saillard, J; Universite de Rennes 1, LCSIM Liu, Chen-Wei; National Dong Hwa University, Chemistry Boucekkine, Abdou; Universit� de Rennes 1, UMR CNRS 6226 Sciences Chimiques de Rennes

Chemical Au-Au bonding induced by UV irradiation of dinuclear Gold(I) complexes. A computational study with experimental evidence.

Authors: Camille Latouche[§&], Yan-Ru Lin[$], Yeny Tobon[#]*, Eric Furet[§], Jean-Yves Saillard[§]*, Chen-Wei Liu[$]*, Abdou Boucekkine[§]*

[§]*Institut des Sciences Chimiques de Rennes, UMR 6226 CNRS-Université de Rennes 1, Campus de Beaulieu, 35042 Rennes cedex, France.*
[&]*Scuola Normale Superiore, Piazza dei Cavalieri 7, I-56126 Pisa, Italy.*
[#]*Laboratoire de Spectrochimie Infrarouge et Raman, UMR 8516 CNRS-Université de Lille 1, Sciences et Technologies, 59655 Villeneuve d'Ascq Cedex, France.*
[$]*Department of Chemistry, National Dong Hwa University, Hualien, Taiwan 97401, Republic of China.*

Abstract:

Two luminescent dinuclear gold(I) species, namely diselenophosphinate $[Au_2\{\mu\text{-}Se_2P(CH_2)_2Ph)_2\}_2]$ and dithiophosphinate $[Au_2\{\mu\text{-}S_2P(CH_2)_2Ph)_2\}_2]$ exhibiting interesting structural, absorption and emission properties have been studied. In the solid state, both complexes exist as a dinuclear monomeric form, exhibiting no aurophilic interaction, and display similar photophysical properties. It is shown, using DFT computations that chemical Au-Au bonding appears in the first excited state of these complexes, whereas such bond does not exist in their ground state; Raman spectroscopy experiments, which bring to light the stretching of this new bond, confirm the theoretical result. Moreover, TDDFT computations permitted to assign the observed absorption bands of the UV-visible spectra of the two species, to LMCT transitions and to describe the emission.

Introduction:

Gold(I) complexes attract a wide range of research groups, mainly due to their large domain of applications, not only in biology but also in the field of sensors and luminescence devices..[1-3] The electronic structure of such complexes is partly driven by relativistic effects. Indeed, the latter effects give rise to a stabilization of the 6s orbitals and a destabilization of the 5d ones [4-7] so that these energy levels become closer than in the cases of Cu(I) or Ag(I) analogues where the relativistic effects are weaker.[8] Such decrease of this energy gap is likely to induce peculiar spectroscopic properties. Another great interest of gold(I) complexes is the presence of d^{10}-d^{10} interaction in dinuclear species as well as their possible aggregation involving the so-called aurophilic interaction for gold(I),[9-11] which has been largely studied from a theoretical point of view by Pyykkö.[4-7] This aurophilic interaction is responsible of the self-assembly of complexes leading to polymers either in the ground state and/or in excited states.[6,10-12]

Previous theoretical studies on multi-nuclear gold(I) complexes, mainly focused on structures and luminescent properties, are reported in the literature.[1,13-15] Herein, we intend to report an investigation of the structural and spectroscopic properties of diselenophosphinate $[Au_2\{\mu\text{-}Se_2P(CH_2)_2Ph)_2\}_2]$ **1** and dithiophosphinate $[Au_2\{\mu\text{-}S_2P(CH_2)_2Ph)_2\}_2]$ **2** dinuclear complexes (Scheme 1). Both species exist under a dinuclear form, even in the solid state, exhibiting large Au-Au distances. In particular, we focus our attention on the possible creation of an Au-Au chemical bond in these species under UV irradiation. To elucidate and prove the existence of such bond in the excited state, a joint experimental and computational study has been undertaken.
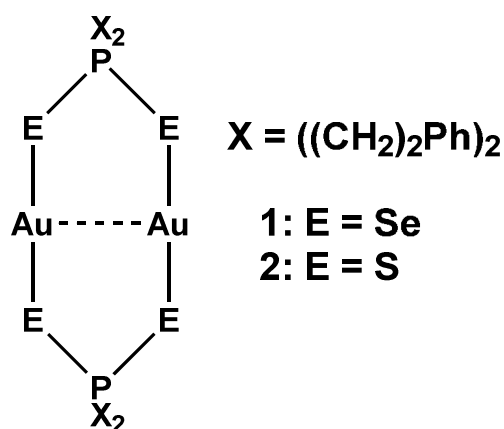
Scheme 1. Studied Complexes

Results and discussion:

The structure as well as the absorption and emission spectra of $[Au_2\{\mu\text{-}Se_2P(CH_2)_2Ph)_2\}_2]$ complex **1** have already been investigated.[12] Among the obtained main results, the computational study brought to light the existence of an Au-Au chemical bond in the excited state which does not exist in the ground state. The experimental confirmation of this phenomenon is presented *vide infra*.

Thus, we found of great interest to undertake a comparative study of $[Au_2\{\mu\text{-}S_2P(CH_2)_2Ph)_2\}_2]$ (complex **2**) and complex **1** in order to check the probable formation of Au-Au chemical bond in the excited state and to evaluate the influence of the chalcogen nature on the properties of these complexes.

The geometry optimization of complex **2** considering THF as solvent (see computational details) has been carried out considering different symmetry constraints and the minimum has been obtained in C_i symmetry for the ground state, the symmetry group which had been already found for complex **1**. Considering the ground state (S_0) the computed structure exhibits an Au-Au distance of 3.32 Å which is in good agreement with the X-ray one (3.27 Å)[16] (Figure 1, Table 1) and a dihedral angle S-Au-Au-S of 180°. Note that the two different observed intramolecular Au-Au distances in the crystal are indicative of important packing effects. The values in Table 1 are similar to the reported data for complex **1** (3.35 Å for the Au-Au distance and 180° for the torsion angle).[12] Furthermore, the computed Au-S distances are slightly overestimating the observed ones (2.35 Å *vs.* 2.29-2.30 Å) whereas the optimized S-P-S angle fits satisfactorily the observed ones (116° *vs.* 117-119°). All optimized coordinates are given in the Supporting Information (SI). The optimized bond lengths and bond angles in the gas phase are similar to those obtained in the THF solvent. In Table 1 are also given optimized geometrical parameters for the first triplet state (T_1) of complex **2**, which will be discussed *vide infra*.
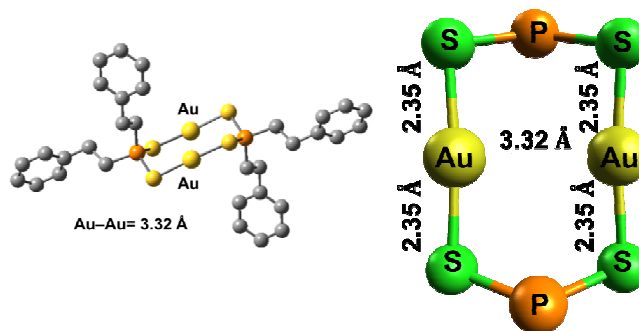

Figure 1. Optimized Ground State Structure of Complex **2** (H atoms are omitted for clarity).

3

Table 1. Relevant X-ray and Computed Geometric Parameters of Complex **2**.

	X-ray [16]	Computed (S$_0$)	Computed (T$_1$)
Au-Au (Å)	3.2668 (2)	3.32	2.65
Au-S (Å)	2.292 (1)	2.35	2*2.37; 2*2.68
S-Au-Au (°)	91.47 (3) - 93.27 (3)	92-93	98-99
S-P-S (°)	118.68 (8)	116 -117	115-116
S-Au-Au-S (°)	180	180	165-166

However, even if the geometries of complexes **1** and **2** are similar, one should notice that the electronic structures are somewhat different. Although the frontier molecular orbitals (MOs) of complexes **2** (Figure 2) and **1** have quite similar plots, complex **2** has a HOMO-LUMO gap of 5.40 eV which is approximately 20% larger than for complex **1** (4.53 eV). The HOMO of **2** is mainly constituted of sulfur lone pairs mixed with $5d_{z^2}$ gold orbital in an out of phase combination, as for complex **1** (with E = Se). The LUMO of complex **2** possesses a strong metal-metal bonding character as for complex **1**, a non-negligible phosphorus character and a less pronounced localization on the chalcogen atoms than that of complex **1** (Figure 2).
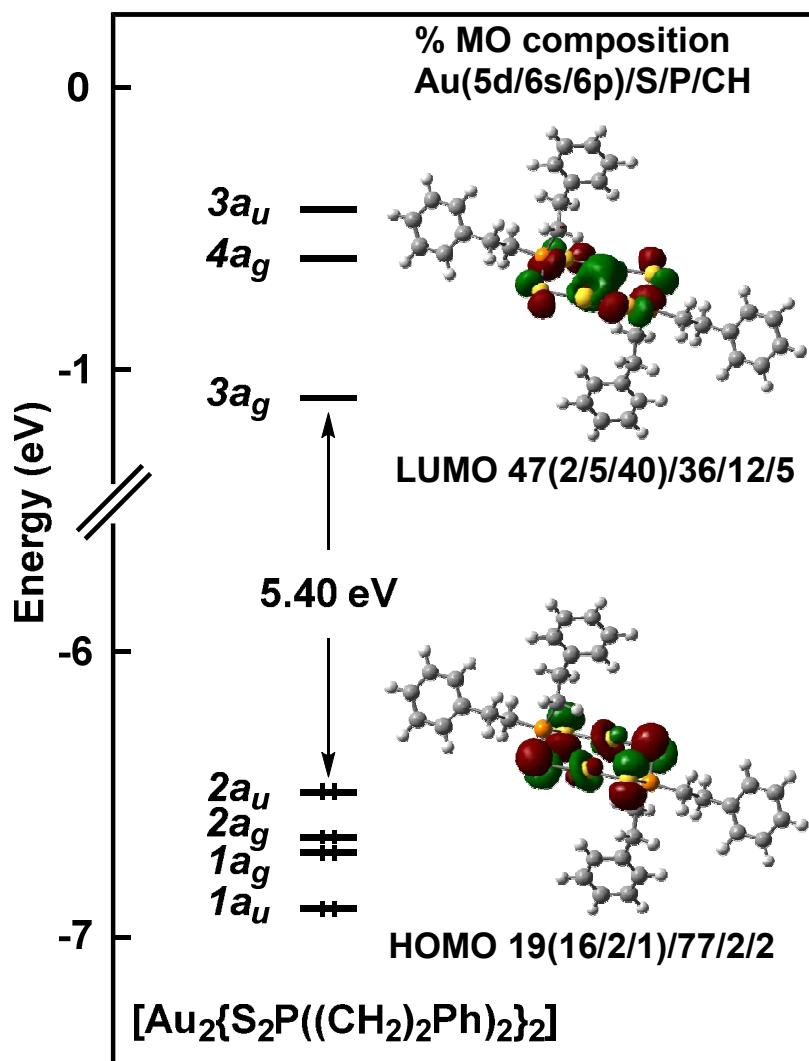
4

% MO composition
Au(5d/6s/6p)/S/P/CH

$3a_u$

$4a_g$

$3a_g$

LUMO 47(2/5/40)/36/12/5

5.40 eV

$2a_u$
$2a_g$
$1a_g$
$1a_u$

HOMO 19(16/2/1)/77/2/2

$[Au_2\{S_2P((CH_2)_2Ph)_2\}_2]$

Figure 2. Frontier MO Diagram of Complex **2**.

If one looks more carefully to the orbital composition, the HOMO of complex **2** is less localized on the chalcogen atoms (77 %) and more on the $5d_{z^2}$ of gold atoms (16 %) than in complex **1** (83 % and 12 % for respectively Se and $5d_{z^2}$).[12] Another difference is also observed considering the localization of the LUMO where the gold 6p contributions are stronger for complex **2** than for complex **1** (40 % *vs.* 28 %) and the chalcogen contributions are weaker (36 % for **2** *vs.* 46 % for **1**).

The excitation and emission spectra of complex **1** have been discussed previously;[12] the spectra of complex **2**, display almost the same features (Table 2, Figure 3). Complex **2** exhibits two structureless bands at 461 nm and 565 nm respectively in the excitation and emission spectra at 298K in the solid state (the UV-visible spectrum of complex **2** is given in

the SI). However, it is necessary to point out that the excitation spectrum in 2-MeTHF at 298K displays a strong bathochromic shift from 324 nm to 356 nm upon the increase of concentration. More intense emission and excitation spectra were detected upon lowering the temperature to 77K. The emission life time (~ 12.9 μs) is indicative of a spin-forbidden triplet excited state.
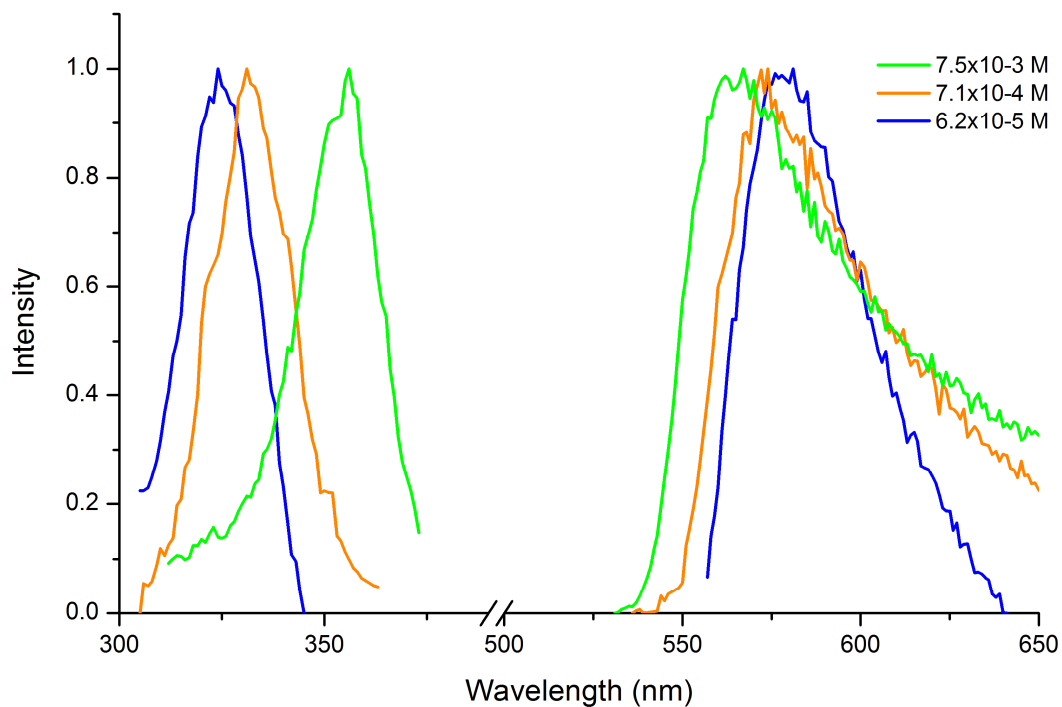

Figure 3: Normalized excitation and emission spectra of complex **2** in 2-MeTHF glass at 298K under different concentrations.

Table 2. Photophysical Data for $[Au_2\{S_2P(CH_2CH_2Ph)_2\}_2]$ complex **2**.

compound	State (T/K)	λ_{max}^{ex}, nm	λ_{max}^{em}, nm	$\tau, \mu s^{b}$
$[Au_2\{S_2P(CH_2CH_2Ph)_2\}_2]$	Solid (298)	461	565	12.9
	Solid (77)	471	565	
	glass^{a} (298)	324 (6.1 x 10^{-5}M)	577	
	(77)	324 (6.1 x 10^{-5}M)	572	
	(298)	331 (7.1 x 10^{-4}M)	572	
	(77)	335 (7.1 x 10^{-4}M)	565	
	(298)	356 (7.5 x 10^{-3}M)	567	
	(77)	360 (7.5 x 10^{-3}M)	558	

^{a}Measured in 2-MeTHF. ^{b}Measured lifetime

Considering the excitation spectra, the probable formation of aggregates, due to the aurophilic interaction, could be responsible for the batochromic shift which is observed at high concentration. This phenomenon has been theoretically investigated in the case of diselenophosphate $[Au_2\{\mu\text{-}Se_2P(CH_2)_2Ph)_2\}_2]$ complexes (R = ^{i}Pr, Et, ^{n}Pr) [12]. However, in the case of complex **2**, the crystal structure does not exhibit any oligomer-like aggregation of the complexes.

The computed absorption wavelength for complex **2** is equal to 293 nm (oscillator strength f = 0.002), with the THF solvent effect taken into account, which compares well with the observed value, 324 nm for the most dilute solution (6.1 × 10^{-5} M concentration). The corresponding transition is mainly a HOMO to LUMO one (percentage weight = 95%). Absorption at shorter wavelengths is computed at ca. 240−260 nm, but the domain range of the measured excitation spectrum is only 280−400 nm, so that no comparison with experimental results could be done. Finally, it must be pointed out that when computing the UV-visible spectrum of a "tetramer" structure of complex **2** derived from the X-ray data, a batochromic shift of the absorption band is observed (absorption at 310 nm instead of 293 nm) bringing to light the importance of environmental effects in this case.

We now consider the first triplet excited state of **2**. Optimization of this excited state geometry has been carried out using unrestricted computations at the same DFT level of theory. The optimized triplet structure of complex **2** is compared to the ground state geometry (Table 1 and Figure 4).

The most important result is that the optimized geometry of the first triplet state of complex **2** exhibits the same very short Au−Au distances as previously obtained for complex **1**, 2.65 Å

vs. 2.69 Å (for respectively complexes **2** and **1**) which represents a shortening of 25 % in comparison to the ground state distance (3.32 Å) (Figure 4). The main structural difference between complexes **2** and **1** is the Au-E (E= S, Se; **2**, **1**) distances. Complex **1** remains in the C_i symmetry in the excited state with all Au-E bond lengths equal; this is not the case for **2**. At the minimum on the energy hypersurface, two Au-S bonds are stretched out from to 2.39 Å to 2.64 Å breaking the symmetry of the complex. More precisely, in the triplet excited state, the C_i structure of complex **2** exhibits an imaginary vibration frequency (i41 cm^{-1}, symmetry A_u). Following this imaginary mode one obtains two energy minima corresponding to geometrically equivalent distorted structures bearing the C_1 symmetry connected to the C_i one, the latter being a transition state (TS) between these two C_1 structures, as shown in Figure 4. The core of the distorted structure has the C_2 symmetry although the full structure exhibits the C_1 symmetry. The difference between the structures of the triplet states of the selenium and sulfur species is probably related to the fact that the Au-S bond is weaker than the Au-Se one, so that distortion is easier for the sulfur complex than for the selenium one. Moreover, since the energy difference between the C_i and C_1 structures of the triplet state of complex **2** is very low (0.4 kcal/mol in the gas phase and 0.8 kcal/mol in THF solution) it is likely that these structures coexist at room temperature. Furthermore, we arrive at the limit of accuracy of the used computational methods. This geometry deformation is unexpected so that we checked it, carrying out several geometry optimizations of the triplet state using different functionals, among them, M062X,[17] MPW1PW91,[18] CAM-B3LYP,[19] which led us to the same result. Moreover, carrying out the optimization of the geometry of this triplet state using TDDFT, led us to almost same results, namely an Au-Au distance equal to 2.652 Å and Au-S distances equal to 2.367 and 2.669 Å. Finally, the latter TDDFT geometry optimization permitted us to estimate the phosphorescence wavelength of this species, *i.e.* 548 nm which compares very well with the observed values at 565 nm (Table 2).
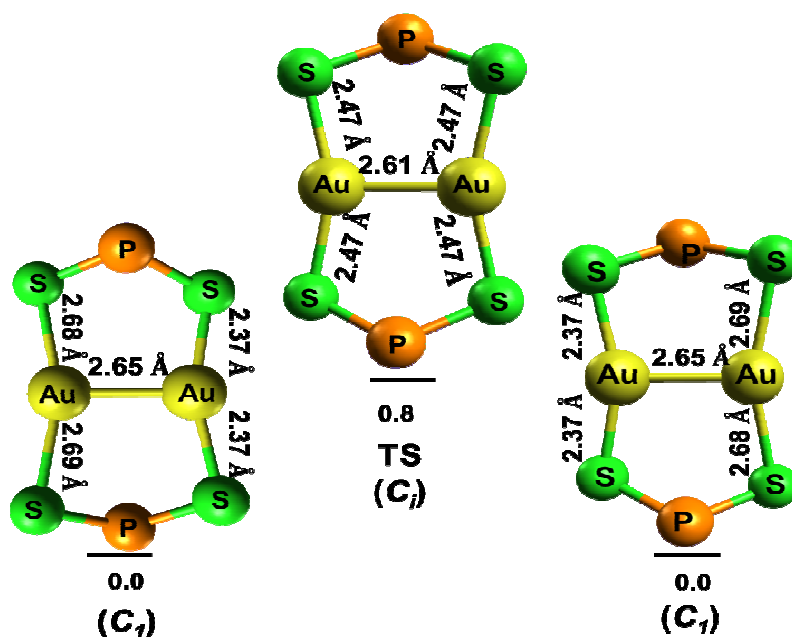
Figure 4. Triplet Excited State (C_i (TS) and C_1) Geometries of Complex **2**. Relative energies in kcal/mol.

This shortening of the Au···Au distance by *ca* 0.5 Å upon excitation to the first triplet state has also been reported by other groups using DFT calculations.[20] Firstly for dinuclear N-heterocyclic dicarbene gold(I) complexes of general formula $[Au_2(RIm-Y-ImR)_2]^-$ $(PF_6)_2$ (R= Me, Cy; Y= $(CH_2)_{1-4}$, o-xylylene, m-xylylene)[21] and, more recently, *Cui et al.* found also photoinduced Gold(I)-Gold(I) chemical bonding in dicyanoaurate oligomers.[20] Such possible shortening of the Au···Au distance in the excited state was already suggested by *Fackler and coworkers* in 1989.[22] This short Au−Au distance is related to the strong Au−Au σ-bonding character of the LUMO (Figure 2) which is indicative of a possible bond formation (formally, a half bond) between the two atoms, in the excited state. This is confirmed by the NBO analysis carried out for the first triplet excited state of complex **2**, which indicates that the Au-Au chemical bonding is ensured by gold *dsp* hybrid orbitals.

In order to confirm the occurrence of Au-Au bonding in the excited state, Raman experiments using different excitation lines have been planned. We remind that DFT computations predict for complex **1** in its triplet state a Au-Au stretching mode at 139 cm^{-1} (130 cm^{-1} in THF solution) which does not exists in the ground state. This stretching mode displays the A_g symmetry, the molecule in both the ground state and triplet excited state exhibiting the C_i symmetry, so that this vibration mode is IR inactive and Raman active. We remind that the

excitation wavelength leading to phosphorescence in the solid state is at 434 nm.[12] Raman spectrum of the solid state complex **1** has been collected using 473, 532 and 633-nm excitation lines. Excitation at 473 nm leads to a Raman spectrum different from the ground state collected with the 532 and 633-nm excitation lines that are far from the resonance condition. Figure 5 shows the Raman spectra collected in resonant (473 nm) and nonresonant conditions (532 and 633 nm). A new band appears in the Raman spectrum of the complex at 135 cm^{-1}, when exciting with 473 nm, which corresponds to the computed value for the Au-Au stretching mode of the excited state at 139 cm^{-1} Conversely, this band is not observed in the ground state as evidenced in the spectra collected far of the resonant condition using the 532 and 633-nm excitations.

Resonance Raman spectroscopy has been used in previous works to study the Au-Au interaction in gold complexes. In these works, Au-Au stretching frequency was observed in the ground and in the excited states.[23,24] It is worth noting that these complexes exhibit short intramolecular Au-Au distances that allow weak metal interaction in the ground state. However, in our study, Au-Au stretch peak was not observed in nonresonant Raman spectra (532 and 633-nm excitation lines). This evidence allows concluding that Au-Au chemical bonding occurs in the excited state only, as predicted by theoretical calculations.

In the same way, Raman experiments have been carried out for the sulfur complex **2** (solid state experimental λ_{ex} = 471 nm). Figure 6 shows the Raman spectra collected in resonant (473 nm) and nonresonant conditions (532 and 633 nm). First of all, a broad luminescence background (relative to the Raman scattering) prevents the analysis of the Raman spectra of the sulfur complex, by using the 633-nm excitation. However, using 473 and 532 nm excitations, we can observe the Raman peaks at low wavenumbers and a new peak around 122 cm^{-1} is observed only when the 473-nm excitation is used. This band is not observed in the ground state as evidenced in the spectrum collected far of the resonant condition using the 532-nm excitation. The DFT computations indicate for an isolated complex that the new Au-Au stretching mode appearing in the triplet state of this complex is at 136 cm^{-1} (same value in THF solution) so permitting us to assign the new band to the formation of the Au-Au chemical bond in the triplet state of complex **2**. Note that in the case of complex **2**, the Au-Au stretching frequency for the C_i structure of the triplet state (transition state) is computed at 155 cm^{-1}, much higher than the observed band at 122 cm^{-1}, thus confirming the distortion of its excited state structure.

These Raman peaks at 135 and 122 cm^{-1} may be assigned, by comparison with the simulated spectra of the ground and excited states of both selenium and sulfur complexes, to the stretching of the Au-Au bond formed in the triplet excited states of these complexes.
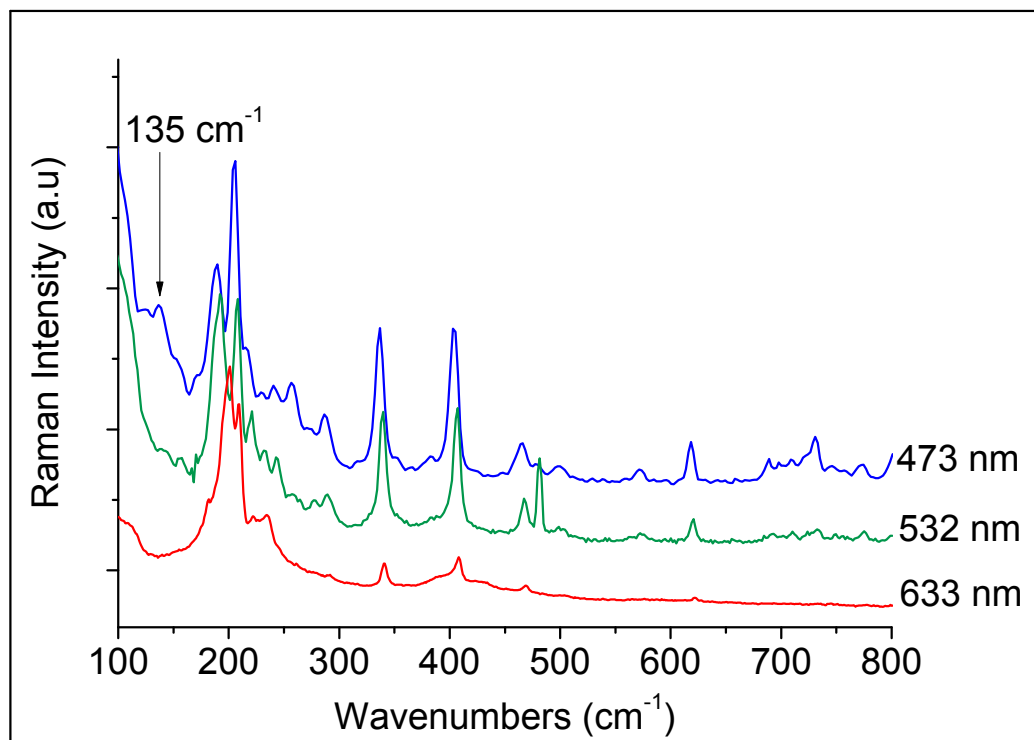

Figure 5. Raman spectra using 473, 532 and 633-nm excitation lines of a solid sample of [Au{μ-Se$_2$P(CH$_2$)$_2$Ph)$_2$}]$_2$ at room temperature, in the 100-800 cm^{-1} region.
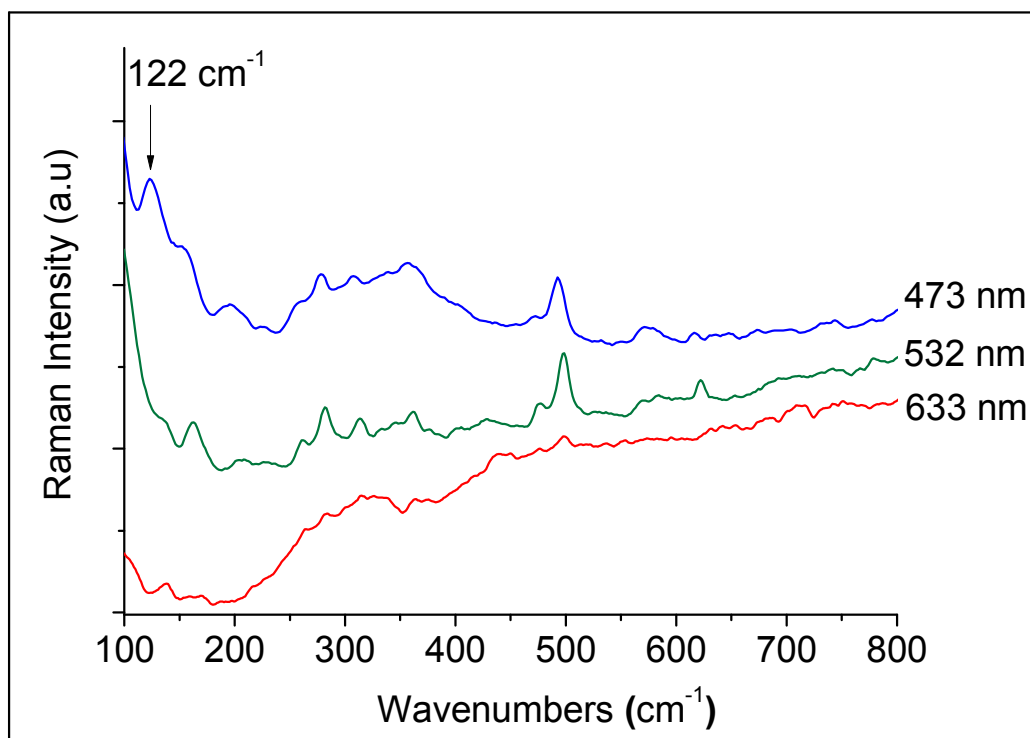
Figure 6. Raman spectra using 473, 532 and 633nm excitation lines of a solid sample of $[Au\{\mu\text{-}S_2P(CH_2)_2Ph)_2\}]_2$ at room temperature, in the 100-800 cm^{-1} region

Conclusions:

The structure and optical properties of two luminescent polynuclear gold(I) species, namely diselenophosphinate $[Au_2\{\mu\text{-}Se_2P(CH_2)_2Ph)_2\}_2]$ **1** and dithiophosphinate $[Au_2\{\mu\text{-}S_2P(CH_2)_2Ph)_2\}_2]$ **2** exhibiting interesting structural, absorption and emission properties have been studied. It is shown, using DFT computations and Raman spectroscopy experiments that Au-Au chemical bonding appears in the first excited triplet state of these complexes whereas such bond does not exist in their ground state. Unexpectedly, it is found that, contrarily to complex **1**, complex **2** undergoes a geometry deformation from the ground state C_i symmetry to the C_1 one, in the triplet state. TDDFT computations permitted to assign the observed absorption bands of the UV-visible spectra; the computed absorption and phosphorescence wavelengths satisfactorily reproduce the observed ones.

Experimental section:

Computational details:

DFT calculations using the PBE0 hybrid functional[25,26] was chosen together with the LanL2DZ basis set[27] augmented with polarizations functions on all atoms, except hydrogen ones. A diffuse "d" orbital (exponent equal to 0.02) has been added on gold atoms. The optimized geometry of the dinuclear complex $[Au_2\{\mu\text{-}S_2P(CH_2)_2Ph)_2\}_2]$ (**2**) has been characterized as true minima on the potential energy surface using vibrational frequency calculations. Then, TDDFT calculations have been performed using the optimized geometry in order to compute the electronic spectra. The optimized geometries of the triplet excited states have been obtained using unrestricted methodology for complex **2**. All computations have been realized considering the complexes either in the gas phase and taking into account the solvent effects (THF), using the PCM model.[28] The program used for the DFT and TDDFT computations was Gaussian 09.[29] Representations of molecular structures and orbitals were done with the Avogadro and Gaussview programs and their compositions have been established using the AOmix software. [30-32]

Photophysical properties:

The photophysical data including excitation, emission, and life time of compounds **2** are summarized in Table 2, and normalized spectra of complex **2** in 2-Me THF glass at 298K under different concentrations are shown in Figure 3. Excitation and emission spectra were recorded on a Cary Eclipse B10 fluorescence spectrophotometer, equipped with an Oxford cryostat (OptistatDN) and a digital temperature controller. Solid samples were prepared in capillary for lifetime studies and the 298 K emission lifetimes was determined by a Edinburgh FLSP920 spectrometer.

Raman Experiments:

The Raman spectra were recorded in the backscattering geometry with a Labram-HR 800 confocal Raman spectrometer (Horiba Scientific), equipped with 600 grooves.mm^{-1} grating, CW 473, 532 and 633-nm lasers, a Liquid Nitrogen-cooled CCD camera and a microscope objective (Olympus BX40; 100×). The powder samples of $[Au_2\{\mu\text{-}Se_2P(CH_2)_2Ph)_2\}_2]$ and $[Au_2\{\mu\text{-}S_2P(CH_2)_2Ph)_2\}_2]$ complexes were placed on a glass slide and positioned directly under the Raman microscope. In order to avoid excessive heating of the sample, we used a

low laser power (~1 mW) and the DuoScant accessory (Horiba Scientific) based on a combination of scanning mirrors that ensure a uniform scanning of the laser beam oven an area of about 100 μm^2. Multiple Raman spectra were averaged to improve signal-to-noise ratio. Low signal/noise ratio was compensated by a long accumulation time.

Supporting Information:
-   Optimized coordinates
-   UV-Visible spectrum of complex **2**

References:

1.   F. Mohr, *Gold Chemistry: Applications and Future Directions in the Life Sciences*, Weinheim, Germany, Wiley-VCH., 2009.

2.   A. Laguna, *Modern Supramolecular Gold Chemistry: Gold-Metal Interactions and Applications*, Weinheim, Germany, Wiley-VCH., 2008.

3.   V. V.-W. Yam and E. C. C. Cheng, *Chem. Soc. Rev.*, 2008, **37**, 1806–1813.

4.   P. Pyykkö and J. P. Desclaux, *Acc. Chem. Res.*, 1979, **12**, 276–281.

5.   P. Pyykkö, *Chem. Rev.*, 1988, **88**, 563–594.

6.   P. Pyykkö, *Angew. Chem. Int. Ed. Engl.*, 2004, **43**, 4412–4456.

7.   P. Pyykkö, *Chem. Soc. Rev.*, 2008, **37**, 1967–1997.

8.   P. Schwerdtfeger, M. Dolg, W. H. E. Schwarz, G. A. Bowmaker, and P. D. W. Boyd, *J. Chem. Phys.*, 1989, **91**, 1762–1774.

9.   S. Sculfort and P. Braunstein, *Chem. Soc. Rev.*, 2011, **40**, 2741-2760

10.   H. Schmidbaur and A. Schier, *Chem. Soc. Rev.*, 2008, **37**, 1931–1951.

11.   H. Schmidbaur and A. Schier, *Chem. Soc. Rev.*, 2012, **41**, 370–412.

12.   C. Latouche, Y.-C. Lee, J.-H. Liao, E. Furet, J.-Y. Saillard, C. W. Liu, and A. Boucekkine, *Inorg. Chem.*, 2012, **51**, 11851–11859.

13.   M.-R. Azani, O. Castillo, M. L. Gallego, T. Parella, G. Aullon, O. Crespo, A. Laguna, S. Alvarez, R. Mas-Ballesté, and F. Zamora, *Chem.—Eur. J.*, 2012, **18**, 9965–9976.

14.   W. E. Van Zyl, J. M. Lopez-de-Luzuriaga, A. A. Mohamed, R. J. Staples, and J. P. Fackler, *Inorg. Chem.*, 2002, **41**, 4579–4589.

15.   O. Elbjeirami, M. W. A. Gonser, B. N. Stewart, A. E. Bruce, M. R. M. Bruce, T. R. Cundari, and M. A. Omary, *Dalt. Trans.*, 2009, 1522.

16.   Y.-C. Lee, Y.-R. Lin, B.-Y. Liou, J.-H. Liao, N. K. Gusarova, B. A. Trofimov, W. E. van Zyl, and C. W. Liu, *Dalt. Trans.*, 2014, **43**, 663–670.

17.   Y. Zhao and D. G. Truhlar, *Theor. Chem. Acc.*, 2007, **120**, 215–241.

18.   C. Adamo and V. Barone, *J. Chem. Phys.*, 1998, **108**, 664–675.

19.   T. Yanai, D. P. Tew, and N. C. Handy, *Chem. Phys. Lett.*, 2004, **393**, 51–57.

20.   G. Cui, X.-Y. Cao, W.-H. Fang, M. Dolg, and W. Thiel, *Angew. Chem. Int. Ed. Engl.*, 2013, **52**, 10281–10285.

21.   M. Baron, C. Tubaro, A. Biffis, M. Basato, C. Graiff, A. Poater, L. Cavallo, N. Armaroli, and G. Accorsi, *Inorg. Chem.*, 2012, **51**, 1778–1784.

22.   C. King, J.-C. Wang, M. N. I. Khan, and J. P. Fackler, *Inorg. Chem.*, 1989, **28**, 2145–2149.

23.   K. H. Leung, D. L. Phillips, M.-C. Tse, C.-M. Che and V. M. Miskowski, *J. Am. Chem. Soc.,* 1999, **121**, 4799-4803.

24.   D. L. Phillips, C. Che, K. H. Leung, Z. Mao, and M. Tse, *Coord. Chem. Rev.*, 2005, **249**, 1476–1490.

25.   C. Adamo and V. Barone, *J. Chem. Phys.*, 1999, **110**, 6158–6169.

26.   M. Ernzerhof and G. E. Scuseria, *J. Chem. Phys.*, 1999, **110**, 5029–5036.

27.   P. J. Hay and W. R. Wadt, *J. Chem. Phys.*, 1985, **82**, 270–283.

28.   J. Tomasi, B. Mennucci, and R. Cammi, *Chem. Rev.*, 2005, **105**, 2999–3094.

29.   Frisch, M. J.; Trucks, G. W.; Schlegel, H. B.; Scuseria, G. E.; Robb, M. A.; Cheeseman, J. R.; Scalmani, G.; Barone, V.; Mennucci, B.; Petersson, G. A.; Nakatsuji, H.; Caricato, M.; Li, X.; Hratchian, H. R.; Izmaylov, A. F.; Bloino, J.; Zheng, G.; Sonnenberg, J. L.; Hada, M.; Ehara, M.; Toyota, K.; Fukuda, R.; Hasegawa, J.; Ishida, M.; Nakajima, T.;

Honda, Y.; Kitao, O.; Nakai, H.; Vreven, T.; Montgomery Jr. J. A. Peralta, J. R.; Ogliaro, F.; Bearpark, M.; Heyd, J. J.; Brothers, E.; Kudin, K. N.; Staroverov, V. N.; Kobayashi, R.; Normand, J.; Raghavachari, K.; Rendell, A.; Burant, J. C.; Iyengar, S. S.; Tomasi, J.; Cossi, M.; Rega, N.; Millam, J. M.; Klene, M.; Knox, J. E.; Cross, J. B.; Bakken, V.; Adamo, C.; Jaramillo, J.; Gomperts, R.; Stratmann, R. E.; Yazyev, O.; Austin, A. J.; Cammi, R.; Pomelli, C.; Ochterski, J. W.; Martin, R. L.; Morokuma, K.; Zakrzewski, V. G.; Voth, G. A.; Salvador, P.; Dannenberg, J. J.; Dapprich, S.; Daniels, A. D.; Farkas, O.; Foresman, J. B.; Ortiz, J. V; Cioslowski, J.; Fox, D. J. *Gaussian09 Revision D01*; 2009.

30.　　M. Hanwell, D. Curtis, D. Lonie, T. Vandermeersch, E. Zurek, and G. Hutchison, *J. Cheminform.*, 2012, **4**, 17.

31.　　Dennington, R.; Keith, T.; Millam, J. GaussView, Version 5, 2009.

32.　　S. I. Gorelsky, *AOMix: Program for Molecular Orbital Analysis*, 2009.
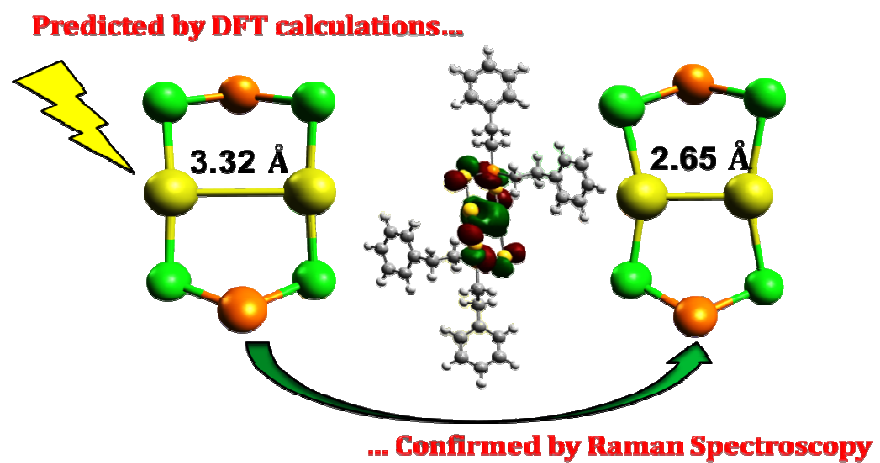
Chemical Au-Au bonding appears upon UV irradiation.